The International Journal of Cardiovascular Imaging (2019) 35:1009–1017
https://doi.org/10.1007/s10554-019-01590-0

ORIGINAL PAPER

The impact of right ventricular function on prognosis in patients with stage III non-small cell lung cancer after concurrent chemoradiotherapy

Lu Chen[1] · Jingjuan Huang[2] · Weihua Wu[1] · Shengjun Ta[3] · Xiaoyi Xie[1]

Received: 6 February 2019 / Accepted: 25 March 2019 / Published online: 2 April 2019

Abstract
Right ventricular (RV) impairment after cancer therapy-related cardiotoxicity and its prognostic implications in lung cancer have not been examined. The present research sought to evaluate RV structure, function, and mechanics in stage III non-small-cell lung cancer (NSCLC) before and after concurrent chemoradiotherapy (CCRT), and to explore the associations between RV impairments, radiation dose, and all-cause mortality. This prospective investigation included 128 inoperable NSCLC patients who were scheduled to receive CCRT. Echocardiographic examination and strain evaluation was performed at baseline and 6 months post-CCRT in all participants. Conventional RV dimensions revealed no significant changes post-CCRT. However, a reduction in RV free wall strain (RV-fwLS) was observed at 6 months post-CCRT ($-28.3 \pm 4.6\%$ vs. $-25.5 \pm 4.8\%$, $P < 0.001$). The same was revealed for global RV longitudinal strain (RV-GLS) ($-23.4 \pm 2.9\%$ vs. $-20.2 \pm 3.4\%$, $P < 0.001$). Pearson correlation showed that RV radiation mean dose was related with the percentage change in RV-fwLS ($r = 0.303$, $P = 0.001$) and RV-GLS ($r = 0.284$, $P = 0.002$). In multivariable analysis, the percentage change in RV-fwLS was an independent predictor of all-cause mortality (HR 1.296, 95% CI 1.202–1.428, $P < 0.001$). RV longitudinal strain is deteriorated at 6 months post-CCRT. The RV mechanics deterioration was associated with radiation dose and affected the long-term outcome of stage III NSCLC patients treated with CCRT.

Keywords Right ventricle · Strain · Chemoradiotherapy · Non-small cell lung cancer

Introduction

Concurrent chemoradiotherapy (CCRT) is the standard treatment for patients with unresectable or medically inoperable stage III non-small-cell lung cancer (NSCLC) [1]. However, thoracic radiotherapy (RT), as the most important component of CCRT, is potentially associated with cardiotoxicity, which has long been recognized in patients with breast cancer [2] or Hodgkin lymphoma [3]. Notably, the data of RT-associated cardiotoxicity for patients with NSCLC is limited. Conventional wisdom holds that there are few long-term NSCLC survivors to experience toxicity, given the typically long latency of RT-associated cardiac injury and poor prognosis. In fact, patients with lung cancer are more likely to have comorbid hazard factors such as advanced age, smoking and probably receive higher heart radiation doses, thus lowering their reserve and predisposing them to earlier cardiac events [4]. In addition, the concurrent use of platinum-based chemotherapy may amplify the cardiotoxic risk [5]. It is therefore important to screen and detect cardiac impairment post-CCRT for NSCLC patients.

Strain imaging is considered a suitable method for early detecting subtle myocardial dysfunction before they are observable by conventional echocardiographic techniques [6]. Multiple studies have validated its role in evaluating cancer treatment-induced left ventricular (LV) subclinical dysfunction and demonstrated the prognostic value of assessing LV myocardial mechanics [7, 8]. Of note, although

Lu Chen and Jinjuan Huang have contributed equally to this work.

✉ Lu Chen
CL2_122@163.com

[1] Department of Ultrasound, Shanghai Chest Hospital, Shanghai Jiao Tong University, 241 Huaihai Road West, Shanghai, China

[2] Department of Cardiology, Shanghai Chest Hospital, Shanghai Jiao Tong University, Shanghai, China

[3] Department of Ultrasound, Yan'an People's Hospital, Yan'an, China

LV dysfunction after cancer treatment have been investigated, the early manifestations of right ventricular (RV) function have not been well characterized, and its incidence and prognostic value in lung cancer patients is unknown. Theoretically, the thinner structure of the RV with lesser myofibrils may make it more vulnerable to cardiotoxicity induced by radiation or chemotherapy [9]. Furthermore, RV is anatomically positioned superficially in the mediastinum, right behind the sternum and ribs, which makes it easily exposed to RT [10]. Considering the fact that RV function have important predictive role in many other cardiovascular diseases [11–13], it would be significant to know if RV impairment is associated with worse outcomes in lung cancer patients. Hence, by using strain imaging, we aimed to study the early effects of CCRT on RV structure, function, and mechanics, and to search for the relationships between the RV impairments and long-term outcome in patients with NSCLC.

Methods

Patients and treatment

A total of 128 patients who had histologically proven and unresectable NSCLC were consecutively enrolled in this study between January 2009 and December 2013. Patients were older than 18 years and had an Eastern Cooperative Oncology Group performance status (ECOG PS) of 0 to 1. All patients were scheduled to receive definitive radiotherapy (RT) with concurrent chemotherapy (57.5% platinum/Taxol doublet, 42.5% platinum/non-Taxol doublet) as tolerated. Exclusion criteria were prior radio- or cardiotoxic chemotherapy, pulmonary hypertension, liver or kidney failure, valvular heart disease (more than mild), malignant pericardial effusions, persistent atrial fibrillation, impaired LV systolic function (LVEF < 50%) and inadequate echocardiographic view. In addition, we calculated the WHO/International Society of Hypertension (WHO/ISH) 10-year mortality risk score to evaluate baseline cardiac risk [14]. This protocol was approved by the institutional review board, and written informed consent was obtained from all patients.

RT doses were prescribed to the planning target volume (PTV). The gross tumor volume was defined as the primary tumor and regionally involved nodes on CT when 1 cm or larger, or standardized uptake values (SUV) > 3. Clinical target volume margins were 0.5–1.0 cm, and PTV margins were 0.5–1.0 cm as well. RT with a median dose of 64.5 Gy (range 53.8–75.3 Gy) and 1.8 or 2.15 Gy per fraction was administered over 5–7 weeks. We employed the dose limits for the heart (V60 Gy < 1/3, V45 Gy < 2/3, and 40 Gy < 100% of the heart). Dose-volume histograms were generated for organs at risk, and parameters for analysis were prespecified largely on the basis of RTOG 0617 [15].

Echocardiography and image analysis

A comprehensive transthoracic echocardiogram was performed at baseline, and 6 months post-CCRT using Vivid 7 or E9 ultrasound scanners (GE Vingmed, Horten, Norway) equipped with a 2.5-MHz broadband transducer. The same ultrasound machine was used to acquire all echocardiograms in each patient. The echocardiographic protocol adhered to the recommendations for chamber quantification of the American Society of Echocardiography [16]. The patients were in the left lateral decubitus position. A simultaneous superimposed ECG was used throughout the studies. Two-dimensional, Doppler and M-mode measurements were performed, and framerate optimized (≥ 50 frames per second) apical 2-, 3-, 4-chamber, and midlevel short axis views were stored for three cycles on the hard drive. All echocardiograms were performed by 2 research sonographers. Measurements were performed by a senior reader who was blinded to the clinical data and outcomes when interpreting the echocardiograms. LV ejection fraction (LVEF) was measured by use of the biplane Simpson's method. RV dimensions were defined as basal, mid-cavity and longitudinal diameter in an apical 4-chamber view. Right atrial (RA) area was estimated by planimetry at the end of ventricular systole (largest atrial volume), tracing the RA endocardium from the lateral aspect of the tricuspid annulus to the septal aspect. Right ventricular end-diastolic area and end-systolic area were measured from the apical four chamber view to calculate RV FAC. To determine TAPSE, M-Mode cursor was placed at the junction of the tricuspid valve plane with the right ventricular free wall, using the images of the apical four-chamber view. Pulmonary artery systolic pressure (PASP) was calculated from the peak continuous-wave Doppler velocity of the tricuspid regurgitation jet plus right atrial pressure, as assessed by the inspiratory collapse of the inferior vena cava.

Peak systolic strain was measured off-line using 2D STE (EchoPAC PC version 10.0; GE Medical Systems). Adequate tracking was controlled by visual inspection, and reanalysis was executed if necessary. Sections with repeated inadequate tracking were excluded from the final results. As conventionally done, RV peak systolic global longitudinal endocardial strain (RV-GLS) was measured from all 6 RV myocardial segments from an apical 4-chamber view (3 segments of the free wall and 3 segments of the interventricular septum) while the RV free wall peak systolic longitudinal strain (RV-fwLS) was obtained from the 3 RV free wall segments only (Fig. 1). This distinction is made since measurement of RV-GLS based on the inclusion of the interventricular septum may

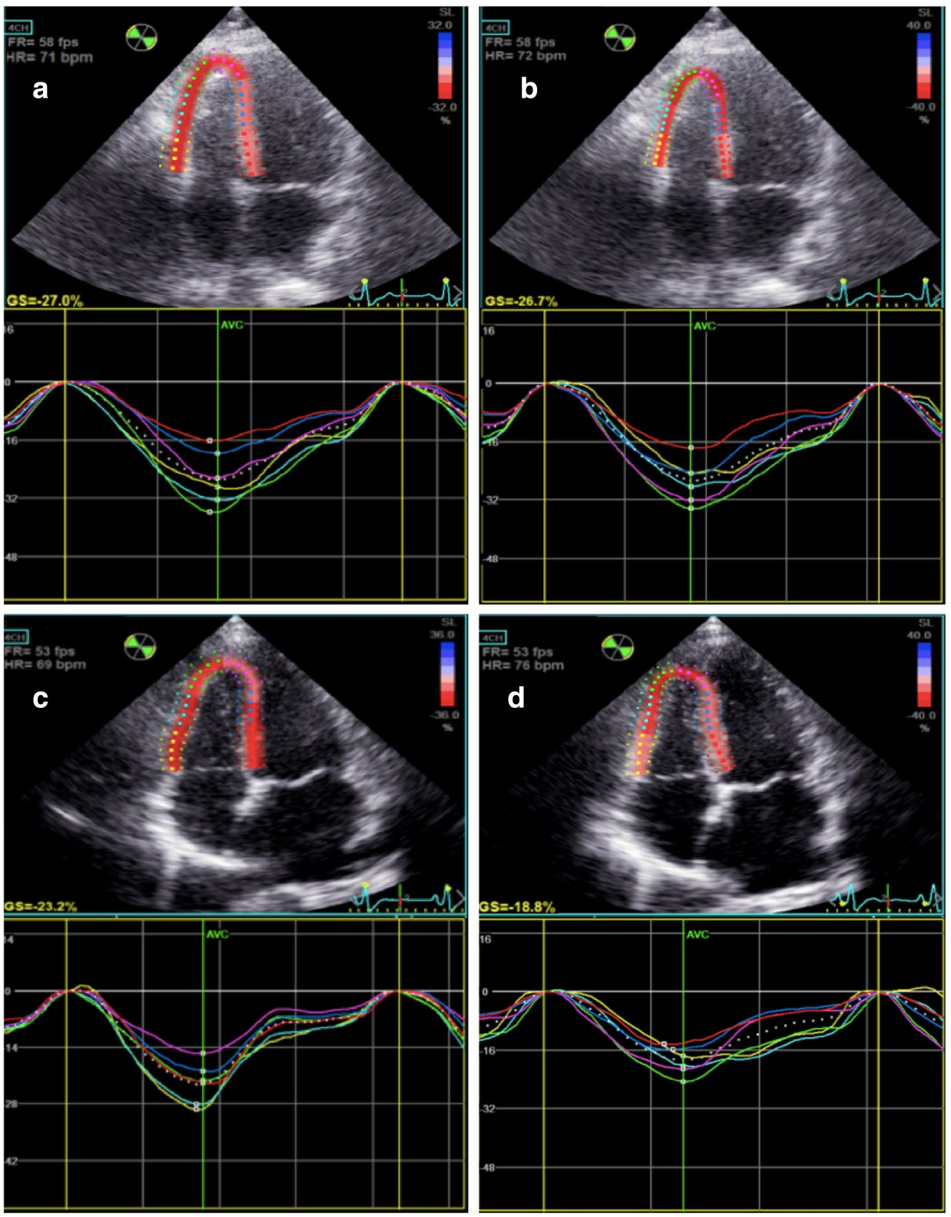

Fig. 1 Example of right ventricular strain measurement from apical 4-chamber view: **a** A good prognosis patient's pre-chemoradiotherapy image depicting right ventricle global (− 27.0%) and free wall longitudinal strain (− 30.1%); **b** the same patient's post-chemoradiotherapy image depicting right ventricle global (− 26.7%) and free wall longitudinal strain (− 29.6%). **c** a poor prognosis patient's pre-chemoradiotherapy image depicting right ventricle global (− 23.2%) and free wall longitudinal strain (− 26.1%); **d** the same patient's post-chemoradiotherapy image depicting right ventricle global (− 18.8%) and free wall longitudinal strain (− 21.6%)

partially reflect changes in the left ventricle as the septum is shared by both ventricles. RV-fwLS focuses only on the RV free wall and does not include contribution of the septum so as to eliminate the influence of left ventricle. The percentage change in RV-fwLS (Δ RV-fwLS %) was calculated between baseline and 6 months post-CCRT.

Follow-up

The primary outcome was all-cause mortality defined as death from any cause occurring at the end of follow-up. All mortality was assessed by reviewing electronic medical records and confirmed by the Social Security Death Index.

Statistical analysis

Continuous data are presented as the mean ± standard deviations, whereas categorical data are presented as percentages. Means were compared using the repeated measurements analysis of variance. Pearson correlation was used to test the linear associations between RV strain changes and RV radiation dose. Intra-observer and inter-observer agreements were calculated using the coefficient of variation (i.e., the absolute percentage difference between the measurements divided by their mean value) and the intraclass correlation coefficient. A Cox, proportional hazards model, was used in the univariable and multivariable analyses to investigate the association between adverse outcomes and clinical

factors. A stepwise variable selection was performed in the multivariable analysis retaining all predictors with P value < 0.05 in the final model. The hazard ratio (HR) and its associated 95% confidence interval (CI) were reported. Receiver operating characteristic (ROC) curve analysis was used to test the value of significant predictors of mortality. The cut-off value was selected as the value corresponding to the highest average of sensitivity and specificity. The cut-off values identified in the above model were then analyzed using the Kaplan–Meier method. To estimate the significance of the Kaplan–Meier curves, the log-rank test was used. P values < 0.05 were considered statistically significant. Statistical analysis was performed with SPSS 18 (SPSS, Chicago, IL).

Results

Baseline characteristics and outcome

The median age was 60 years (range 40 to 79 years); 31.3% of the patients were aged 70 years and older. The majority (65.6%) of patients were male; 59.4% had an ECOG PS score of 0; slightly more patients had stage IIIA disease (53.1%); 73.4% had non-squamous histology; 45.3% had WHO/ISH 10-year risk scores > 10. Most patients (87.5%) had been treated with 3D CRT, and the other 16 patients (12.5%) received IMRT. The median, mean radiation dose was 65.5 Gy (range 60 to 70 Gy), and RV mean dose was 4.2 Gy (range 1.2 to 8.6 Gy). The detailed baseline characteristics of the patients are shown in Table 1.

The median follow-up period was 34 months (range 7–61 months), and no patients were lost to follow-up. The median OS was 27.5 months, and the 2- and 3-year OS were 47.7% and 32.5%, respectively.

Echocardiographic parameters

Neither the LV nor the RV dimensions specifically changed in the sequential follow-up (all P > 0.05). Compared with baseline, LVEF remained unchanged at 6 months after CCRT (P > 0.05). Whereas E/e' presented a significant increase (P = 0.01), which implied a progression of LV diastolic dysfunction. Traditional parameters of RV longitudinal function (FAC, TAPSE and s') revealed no significant changes (all P > 0.05).

Totally, 702 of 768(91.4%) RV segments were successfully analyzed by strain imaging, and the number of losing tracking segments was less than 15%. The absolute value of RV-fwLS (−28.3 ± 4.6% vs. −25.5 ± 4.8%, P < 0.001) and RV-GLS (−23.4 ± 2.9% vs. −20.2 ± 3.4%, P < 0.001) were significantly reduced at 6 months post-CCRT (Table 2).

Table 1 Baseline Patient clinical characteristics

Characteristics	Prevalence
Age (years)	
18–59	28 (21.8%)
60–69	60 (46.9%)
70–79	40 (31.3%)
Sex	
Male	84 (65.6%)
Female	44 (34.4%)
ECOG PS score, n(%)	
0	76 (59.4%)
1	52 (40.6%)
Clinical stage, n(%)	
IIIA	68 (53.1%)
IIIB	60 (46.9%)
Tumor stage	
0/1	29 (22.7%)
2	43 (33.6%)
3	33 (25.7%)
4	23 (18.0%)
Node stage	
0/1	8 (6.3%)
2	83 (64.8%)
3	37 (28.9%)
Histology, n (%)	
Squamous	34 (26.6%)
Non-squamous	94 (73.4%)
WHO/ISH 10-year risk, n (%)	
0 to < 10	70 (54.7%)
10 to < 20	41 (32.0%)
≥ 20	17 (13.3%)
Smoking status	
Non-smoker	40 (31.3%)
Ex-smoker, smoker	88 (68.7%)
Radiation technique	
IMRT	16 (12.5%)
3D CRT	112 (87.5%)
PTV, cm^3, median (range)	446.6 (98.9–868.8)
Prescribed RT dose, Gy median (range)	65.5 (60–70)
Heart mean dose, Gy median (range)	13.3 (7.8–18.8)
RV mean dose, Gy median (range)	4.2 (1.2–8.6)
Lung mean dose,Gy median (range)	18.9 (15.5–21.3)

ECOG PS Eastern Cooperative Oncology Group performance status, *WHO/ISH* WHO/International Society of Hypertension, *IMRT* intensity-modulated radiotherapy, *3D CRT* three-dimensional conformal radiotherapy, *PTV* planning target volume, *RV* right ventricle

The mean percentage changes in RV-fwLS (ΔRV-fwLS %) and RV-GLS (ΔRV-GLS %)from baseline to 6 months after CCRT were 10.1 ± 3.1% and 12.9 ± 2.9%, respectively.

Table 2 Echocardiographic parameters

Parameter	Baseline	After 6 months	*P* value
LV measurements			
LVEDd (mm)	46.1 ± 3.2	46.4 ± 3.8	0.495
LVESd (mm)	25.7 ± 2.7	25.8 ± 2.8	0.771
LVEDV (ml)	101.1 ± 14.5	102.0 ± 14.4	0.618
LVESV (ml)	38.4 ± 8.5	39.1 ± 8.2	0.503
LVEF (%)	61.2 ± 6.8	60.7 ± 6.6	0.551
E/e′	9.9 ± 1.4	12.8 ± 1.8	0.010
RV measurements			
RV basal diameter (mm)	33.8 ± 4.5	34.3 ± 4.8	0.391
RV mid diameter (mm)	28.5 ± 3.5	29.2 ± 3.3	0.101
RV longitudinal diameter (mm)	70.1 ± 6.1	70.9 ± 5.7	0.279
RA area (cm^2)	14.2 ± 2.2	14.6 ± 2.4	0.166
PASP (mmHg)	33.5 ± 4.2	35.6 ± 4.9	0.004
FAC (%)	46.5 ± 4.6	45.9 ± 4.2	0.277
TAPSE (cm)	21.3 ± 2.9	20.9 ± 2.6	0.246
RV s′ (cm/s)	11.5 ± 2.4	11.3 ± 2.5	0.514
RV-GLS (%)	23.4 ± 2.9	20.2 ± 2.4	< 0.001
RV-fwLS (%)	28.3 ± 2.6	25.5 ± 2.8	< 0.001

Data are presented as the mean ± SD

LVEDd left ventricular end diastolic diameter, *LVESd* left ventricular end systolic diameter, *LVEDV* left ventricular end-diastolic volume, *LVESV* left ventricular end-systolic volume, *LVEF* left ventricular ejection fraction, *E* early diastolic mitral flow (pulsed Doppler), *e'* average of the peak early diastolic relaxation velocity of the septal and lateral mitral annulus (tissue Doppler), *RV* right ventricle, *RA* right atrium, *PASP* Pulmonary artery systolic pressure, *FAC* fractional area change, *TAPSE* tricuspid annular plane systolic excursion, *s′* peak systolic velocity of the tricuspid annulus, *GLS* global longitudinal strain, *fwLS* free wall longitudinal strain

Associations between RV strain changes and radiation dose

A modest correlation was observed between the changes of RV strain and radiation doses to the corresponding cardiac structures. ΔRV-GLS % correlated with the heart mean dose (r = 0.284, P = 0.002), the RV mean dose (r = 0.347, P < 0.001) and the RV free wall mean dose (r = 0.303, P = 0.001). ΔRV-fwLS % correlated with the heart mean dose (r = 0.260, P = 0.006), the RV mean dose (r = 0.291, P = 0.002) and the RV free wall mean dose (r = 0.395, P < 0.001).

Intra-observer and inter-observer variability

The intra-observer and inter-observer variabilities for RV-fwLS were 4.4% ± 1.8% and 5.7% ± 1.6%, respectively. The interclass correlation coefficients were 0.91 and 0.86 for intra-observer and inter-observer RV-fwLS measurements, respectively.

Predictors of all-cause mortality

Only variables yielding values of p < 0.25 and exhibiting significant trends in the univariate analysis were included in the multivariate analysis. These variables were age, tumor stage, node stage, histology, PTV, radiation dose, PASP, RV-fwLS at baseline and ΔRV-fwLS %. Multivariable analysis showed that age (HR 3.312, 95% CI 1.850–6.268, P = 0.003), tumor stage (HR 4.324, 95% CI 2.250–8.268, P < 0.001), and PTV (HR 2.049, 95% CI 1.154–3.861, P = 0.001) were significant predictors of all-cause mortality. Among echo parameters, RV-fwLS at baseline (HR 1.391, 95% CI 1.312–1.678, P < 0.001) and ΔRV-fwLS % (HR 1.296, 95% CI 1.202–1.428, P < 0.001) proved to be independent predictors of all-cause mortality (Table 3).

Based on ROC analysis, ΔRV-fwLS (%) ≥ 10.1% had 62.2% sensitivity and 71.1% specificity for predicting of mortality in NSCLC patients (AUC 0.729, 95% CI 0.643–0.803, P < 0.001, Fig. 2). The ΔRV-fwLS (%) data ranked according to the ROC analysis were used for survival estimation via the Kaplan–Meier method. Figure 3 show the OS estimates for patients stratified by ΔRV-fwLS % cut-off value. The differences in OS were statistically significant (log-rank test, P < 0.001). The mean survival time was 39.2 months (95% CI 34.71–43.72) and 16.7 months (95% CI 13.45–20.11) for the low ΔRV-fwLS% and high ΔRV-fwLS% groups, respectively.

Conclusion

There are three main findings of the present study: (i) RV-fwLS, and RV-GLS were significantly reduced at 6 months post-CCRT, while conventional RV echocardiographic parameters remained unchanged; (ii) There was a modest correlation between the reduction of RV strain and radiation dose; (iii) Independent of other parameters, RV-fwLS at baseline and its change post-CCRT significantly correlated with all-cause mortality of stage III NSCLC patients.

RV has long been regarded as the forgotten side of the heart and only a few attention has been paid to its evaluation after RT. Tuohinen et al. [17, 18], showed that the RV free wall was actually exposed to a higher dose than the LV (4.61 vs. 4.37 Gy) in women with left-sided breast cancer, but no deterioration in conventional RV echocardiographic measures was found after RT. However, Christiansen et al. [19] and Murbraech et al. [20] found significantly impaired RV systolic function (assessed by TAPSE, FAC and s') in long-term Lymphoma survivors who received mediastinal RT compared with controls after more than 10 years of diagnosis. In the present study, conventional RV dimensions and longitudinal function did not show significant changes post-CCRT in NSCLC patients. This implies that conventional

Table 3 Cox regression analysis for all-cause mortality

Variable	Univariable			Multivariable		
	HR	95% CI	*P*	HR	95% CI	*P*
General						
Age	3.117	2.013–4.824	< 0.001	3.312	1.850–6.268	0.003
Male sex	1.010	0.484–2.107	0.978			
ECOG PS score	1.192	0.779–1.826	0.418			
T stage T0/1/2 vs. T3/4	4.795	2.991–7.686	< 0.001	4.324	2.250–8.268	< 0.001
N stage N0/1/2 vs. N3	4.958	3.100–7.930	< 0.001			
Histology	1.959	1.266–3.033	0.003			
PTV	3.124	1.925–5.071	< 0.001	2.049	1.154–3.861	0.001
Radiation dose	1.663	1.142–2.682	0.010			
Echo parameters						
PASP	1.032	1.012–1.965	0.002			
FAC	1.004	0.914–1.102	0.938			
TAPSE	0.981	0.881–1.092	0.723			
RV s′	0.948	0.864–1.039	0.254			
RV-fwLS	1.455	1.308–1.619	< 0.001	1.391	1.312–1.678	< 0.001
ΔRV-fwLS %	1.311	1.213–1.417	< 0.001	1.296	1.202–1.428	< 0.001

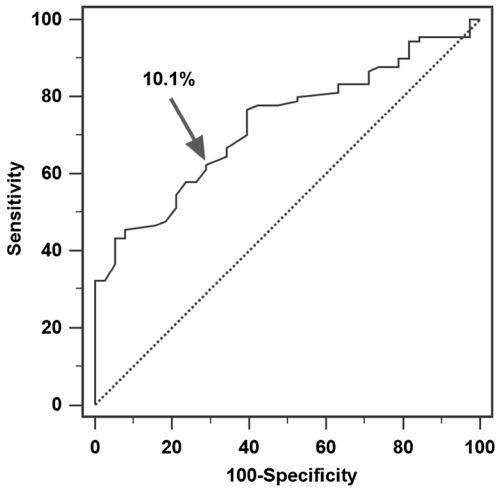

Fig. 2 Receiver Operating characteristic (ROC) curve analysis identified ΔRV-fwLS % 10.1% as optimal cut-off point to predict all-cause mortality in stage III NSCLC patients with a sensitivity of 62.2%, specificity of 71.1% and area under the curve (AUC) of 0.729 (95% CI 0.643–0.803, P < 0.001)

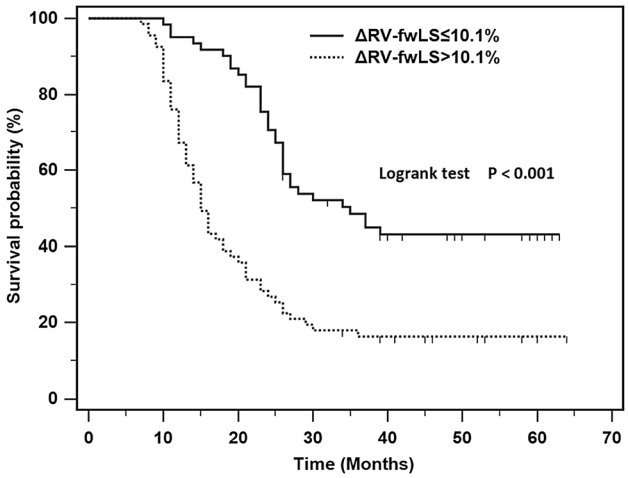

Fig. 3 Kaplan-Meier overall survival curves for patients with stage III NSCLC dichotomized by ΔRV-fwLS % after CCRT greater than/equal to or less than 10.1% (log-rank test, P < 0.001)

RV echocardiographic parameters could be successfully used in the long-term follow-up, but not sensitive enough in detection of occult RV dysfunction at early stage after RT.

Our study revealed that RV longitudinal strain of the entire RV, as well as isolated RV free wall, were significantly reduced in NSCLC patients receiving CCRT. Similarly, several studies demonstrated significant worsening of RV longitudinal strain during and after chemotherapy in breast cancer patients [21–23]. These findings indicate that RV longitudinal strain is a sensitive parameter of RV function that could detect subtle changes at subclinical levels after cancer therapy. Unlike the LV strain that can be subdivide by longitudinal, circumferential and radial direction, the RV strain mostly refers to the evaluation of the longitudinal strain [24]. RV fibers in the endocardial layer are predominately oriented in the longitudinal direction, and their shortening is mainly responsible for the RV ejection [25]. RV impairment is characterized by progressive reduction of longitudinal function

with preserved and even increased transversal function due to circumferential fibers of the epicardial layer at an early stage [26]. Therefore, although FAC remains within the normal range which reflect RV radial function, RV longitudinal strain could be already deteriorated.

Our study found that the decrease of RV longitudinal strain was significantly associated with RV mean dose, indicating that the deterioration of RV mechanics may be caused by the effects of radiation. The mechanisms of inducing RV impairment during and after RT are multifactorial and not fully understood. The main cause could be RT-induced myocardial endothelial injury and microcirculatory obstruction [27, 28]. Another crucial factor that should not be ignored is RT-induced lungs and interstitial pulmonary fibrosis [29]; RT-induced endothelial damage and inflammation could also occur in the pulmonary microcirculation [30]. Both mechanisms could result in an increase in pulmonary resistance and pulmonary wedge pressure, which may raise pulmonary pressure and eventually cause or worsen RV dysfuncion. Moreover, indirect effects of various cytokines that cancer produces could initiate cardiac dysfunction [31]. Recent study reported that RV mechanics was impaired in chemo- and radiotherapy-naïve cancer patients, implying the existence of so-called cancer-induced cardiotoxicity [32]. Potential RV mechanics impairment at baseline may make it more vulnerable to the effects of radiation.

It should be noted that concurrent use of Platinum-based chemotherapy may multiply the cardiotoxicity. Hatakenaka et al. [33] found that Platinum-based CCRT for esophageal cancer impairs cardiac function from an early treatment stage, and this impairment is prominent in the high radiation dose group. The pathophysiology is multifactorial, including procoagulant and direct endothelial toxic effects. Haugnes et al. [34] reported that Platinum-treated survivors of testicular cancer have unfavorable cardiovascular risk status and a higher incidence of cardiovascular event. Platinum-based therapies are also known to increase the risk of thrombus formation [35].

Furthermore, our study suggested that RV-fwLS at baseline was a powerful predictor of all-cause mortality. To the best of our knowledge, this is the first study to show prognostic value of RV longitudinal strain in lung cancer patients. Of course, RV-fwLS is not the only parameter with significant influence on adverse outcome and should be evaluated in the context with other clinical parameters. Not surprisingly, RV-fwLS as a marker of longitudinal RV function is associated with mortality. In contrast, conventional functional parameters such as FAC do not have a similar predictive power as shown in the multivariable Cox regression analysis. RV longitudinal strain is a useful predictor of morbidity and mortality in patients with different conditions—heart failure, cardiomyopathies, pulmonary hypertension, congenital heart diseases, pulmonary fibrosis, and valvular diseases [11, 12, 36–39]. Our study sought to expand current knowledge by assessing the impact of RV mechanics on all-cause mortality in a cohort of patients with NSCLC. Interestingly, the change of RV-fwLS at 6 months post-CCRT also correlated with all-cause mortality. And the patients who had a $\geq 10.1\%$ decrease in RV-fwLS were likely to have worse prognosis than those with lower decrease RV-fwLS. The findings may imply that the impaired RV function, even occult, may remarkably affect the cardiopulmonary function which is crucial to survival of lung cancer patients. Although clinical deterioration did not occur in a relatively short time, this investigation may give rise to attention to the right heart function in lung cancer patients. Thus, the assessment of RV mechanics is necessary and should be considered as the part of follow-up evaluation of NSCLC patients treated with CCRT.

Limitations

We recognize several limitations of this study. First, the size of the patient population was relatively small, which might limit the clinical implications of the results. The second limitation was the technical defects of STE, which might have biased the patient selection. For example, we had to focus on inpatients with good-quality images, thus limiting the generalizability of our findings. Third, RV strain values are still vendor dependent due to the use of different algorithms. The differences are slight but statistically significant and, thus, must be taken into account. Finally, since all-cause mortality was assessed, we could not imply the results of our study to cardiovascular mortality in NSCLC patients.

Conclusions

The present investigation revealed that RV longitudinal strain was impaired post-CCRT, and the deterioration of RV mechanics was associated with radiation dose. The percentage change of RV free wall was an independent predictor of all-cause mortality of stage III NSCLC patients. These findings should encourage physicians to monitor RV function after cancer treatment.

Acknowledgements This work was supported by the Shanghai Charity Cancer Research Center [Grant No. SCCRC17004].

Conflict of interest All authors declare no conflicts of interest.

References

1. Auperin A, Le Pechoux C, Rolland E, Curran WJ, Furuse K, Fournel P, Belderbos J, Clamon G, Ulutin HC, Paulus R, Yamanaka T,

Bozonnat MC, Uitterhoeve A, Wang XF, Stewart L, Arriagada R, Burdett S, Pignon JP (2010) Meta-analysis of concomitant versus sequential radiochemotherapy in locally advanced non–small-cell lung cancer. J Clin Oncol 28(13):2181–2190
2. Aleman BM, van den Belt-Dusebout AW, De Bruin ML, van't Veer MB, Baaijens MH, de Boer JP, Hart AA, Klokman WJ, Kuenen MA, Ouwens GM, Bartelink H, van Leeuwen FE (2007) Late cardiotoxicity after treatment for Hodgkin lymphoma. Blood 109:1878–1886
3. Hooning MJ, Botma A, Aleman BM, Baaijens MH, Bartelink H, Klijn JG, Taylor CW, van Leeuwen FE (2007) Long-term risk of cardiovascular disease in 10-year survivors of breast cancer. J Natl Cancer Inst 99:365–375
4. Wang K, Eblan MJ, Deal AM, Lipner M, Zagar TM, Wang Y, Mavroidis P, Lee CB, Jensen BC, Rosenman JG, Socinski MA, Stinchcombe TE, Marks LB (2017) Cardiac toxicity after radiotherapy for stage III non–small-cell lung cancer: pooled analysis of dose-escalation trials delivering 70 to 90 Gy. J Clin Oncol 35:1387–1394
5. Wachters FM, Van Der Graaf WT, Groen HJ (2017) Cardiotoxicity in advanced non-small cell lung cancer patients treated with platinum and non-platinum based combinations as first-line treatment. Anticancer Res 24:2079–2083
6. Mor-Avi V, Lang RM, Badano LP, Belohlavek M, Cardim NM, Deru-meaux G, Galderisi M, Marwick T, Nagueh SF, Sengupta PP, Sicari R, Smiseth OA, Smulevitz B, Takeuchi M, Thomas JD, Vannan M, Voigt JU, Zamorano JL (2011) Current and evolving echocardiographic techniques for the quantitative evaluation of cardiac mechanics: ASE/EAE consensus statement on methodology and indication sendorsed by the Japanese Society of Echocardiography. J Am Soc Echocardiogr 24:277–313
7. Negishi K, Negishi T, Hare JL, Haluska BA, Plana JC, Marwick TH (2013) Independent and incremental value of deformation indices for prediction of trastuzumab-induced cardiotoxicity. J Am Soc Echocardiogr 26:493–498
8. Mele D, Malagutti P, Indelli M, Ferrari L, Casadei F, Da Ros L, Pollina A, Fiorencis A, Frassoldati A, Ferrari R (2016) Reversibility of left ventricle longitudinal strain alterations induced by adjuvant therapy in early breast cancer patients. Ultrasound Med Biol 42:125–132
9. Tanindi A, Demirci U, Tacoy G, Buyukberber S, Alsancak Y, Coskun U, Yalcin R, Benekli M (2011) Assessment of right ventricular functions during cancer chemotherapy. Eur J Echocardiogr 12:834–840
10. Groarke JD, Nguyen PL, Nohria A, Ferrari R, Cheng S, Moslehi J (2014) Cardiovascular complications of radiation therapy for thoracic malignancies: the role for non-invasive imaging for detection of cardiovascular disease. Eur Heart J 35:612–623
11. Guendouz S, Rappeneau S, Nahum J, Dubois-Rande J-L, Gueret P, Monin J-L, Lim P, Adnot S, Hittinger L, Damy T (2012) Prognostic significance and normal values of 2D strain to assess right ventricular systolic function in chronic heart failure. Circ J 76:127–136
12. Iacoviello Iacoviello M, Citarelli G, Antoncecchi V, Romito R, Monitillo F, Leone M, Puzzovivo A, Lattarulo MS, Rizzo C, Caldarola P, Ciccone MM (2016) Right ventricular longitudinal strain measures independently predict chronic heart failure mortality. Echocardiography 33:992–1000
13. Gulati A, Ismail TF, Jabbour A, Alpendurada F, Guha K, Ismail NA, Raza S, Khwaja J, Brown TDH, Morarji K, Liodakis E, Roughton M, Wage R, Pakrashi TC, Sharma R, Carpenter JP, Cook SA, Cowie MR, Assomull RG, Pennell DJ, Prasad SK (2013) The prevalence and prognostic significance of right ventricular systolic dysfunction in nonischemic dilated cardiomyopathy. Circulation 128:1623–1633
14. Mendis S, Lindholm LH, Mancia G, Whitworth J, Alderman M, Lim S, Heagerty T (2007) World Health Organization (WHO) and International Society of Hypertension (ISH) risk prediction charts: assessment of cardiovascular risk for prevention and control of cardiovascular disease in low and middle-income countries. J Hypertens 25:1578–1582
15. Bradley JD, Paulus R, Komaki R, Masters G, Blumenschein G, Schild S, Bogart J, Hu C, Forster K, Magliocco A, Kavadi V, Garces YI, Narayan S, Iyengar P, Robinson C, Wynn RB, Koprowski C, Meng J, Beitler J, Gaur R, Curran W Jr, Choy H (2015) Standard-dose versus high-dose conformal radiotherapy with concurrent and consolidation carboplatin plus paclitaxel with or without cetuximab for patients with stage IIIA or IIIB non-small-cell lung cancer (RTOG 0617): a randomised, two-by-two factorial phase 3 study. Lancet Oncol 16:187–199
16. Lang RM, Badano LP, Mor-Avi V, Afilalo J, Armstrong A, Ernande L, Flachskampf FA, Foster E, Goldstein SA, Kuznetsova T, Lancellotti P, Muraru D, Picard MH, Rietzschel ER, Rudski L, Spencer KT, Tsang W, Voigt JU (2015) Recommendations for cardiac chamber quantification by echocardiography in adults: an update from the American Society of Echocardiography and the European Association of Cardiovascular Imaging. Eur Heart J Cardiovasc Imaging 16:233–270
17. Tuohinen SS, Skyttä T, Virtanen V, Virtanen M, Luukkaala T, Kellokumpu-Lehtinen PL, Raatikainen P (2016) Detection of radiotherapy-induced myocardial changes by ultrasound tissue characterisation in patients with breast cancer. Int J Cardiovasc Imaging 32:767–776
18. Tuohinen SS, Skyttä T, Poutanen T, Huhtala H, Virtanen V, Kellokumpu-Lehtinen PL, Raatikainen P (2017) Radiotherapy-induced global and regional differences in early stage left-sided versus right-sided breast cancer patients: speckle tracking echocardiography study. Int J Cardiovasc Imaging 33:463–472
19. Christiansen JR, Massey R, Dalen H, Kanellopoulos A, Hamre H, Ruud E, Kiserud CE, Fossa SD, Aakhus S (2016) Right ventricularfunction in long-term adult survivors of childhood lymphomaand acute lymphoblastic leukaemia. Eur Heart J Cardiovasc Imaging 17:735–741
20. Murbraech K, Holte E, Broch K, Smeland KB, Holte H, Rosner A, Lund MB, Dalen H, Kiserud C, Aakhus S (2016) Impaired right ventricularfunction in long-term lymphoma survivors. J Am Soc Echocar-diogr 29:528–536
21. Boczar KE, Aseyev O, Sulpher J, Johnson C, Burwash IG, Turek M, Dent S, Dwivedi G (2016) Right heart function deteriorates in breast cancer patients undergoing anthracycline-based chemotherapy. Echo Res Pract 3:79–84
22. Calleja A, Poulin F, Khorolskym C, Shariat M, Bedard PL, Amir E, Rakowski H, McDonald M, Delgado D, Thavendiranathan P (2015) Right ventricular dysfunction in patients experiencing cardiotoxicity during breast cancer therapy. J Oncol 2015:609194
23. Chang WT, Shih JK, Feng YH, Chiang CY, Kuo YH, Chen WY, Wu HC, Cheng JT, Wang JJ, Chen ZC (2016) The early predictive value of right ventricular strain in epirubicin-induced cardiotoxicity in patients with breast cancer. Acta Cardiol Sin 32:550–559
24. Ozawa K, Funabashi N, Tanabe N, Tatsumi K, Kobayashi Y (2016) Contribution of myocardial layers of right ventricular free wall to right ventricular function in pulmonary hypertension: analysis using multilayer longitudinal strain by two-dimensional speckle-tracking echocardiography. Int J Cardiol 215:457–462
25. Kukulski T, H¨ubbert L, Arnold M, Wranne B, Hatle L, Sutherland GR (2000) Normal regional right ventricular function and its change with age: a Doppler myocardial imaging study. J Am Soc Echocardiogr 13:194–204
26. Torrent-Guasp F, Ballester M, Buckberg GD, Carreras F, Flotats A, Carrió I, Ferreira A, Samuels LE, Narula J (2001) Spatial

orientation of the ventricular muscle band: physiologic contribution and surgical implications. J Thorac Cardiovasc Surg 122:389–392
27. Burger A, Loffler H, Bamberg M, Rodemann HP (1998) Molecular and cellular basis of radiation fibrosis. Int J Radiat Biol 73:401–408
28. Taunk NK, Haffty BG, Kostis JB, Goyal S (2015) Radiation-induced heart desease: pathologic abnormalities and putative mechanisms. Front Oncol 5:39
29. Chen Z, Wu Z, Ning W (2019) Advances in molecular mechanisms and treatment of radiation-induced pulmonary fibrosis. Transl Oncol 12:162–169
30. Abratt RP, Morgan GW, Silvestri G, Willcox P (2004) Pulmonary complications of radiation therapy. Clin Chest Med 25:167–177
31. Padrão AI, Moreira-Gonçalves D, Oliveira PA, Teixeira C, Faustino-Rocha AI, Helguero L, Vitorino R, Santos LL, Amado F, Duarte JA, Ferreira R (2015) Endurance training prevents TWEAK but not myostatin-dediated cardiac remodelling in cancercachexia. Arch Biochem Biophys 567:13–21
32. Tadic M, Baudisch A, Haßfeld S, Heinzel F, Cuspidi C, Burkhardt F, Escher F, Philipp A, Pieske B, Genger M (2018) Right ventricular function and mechanics in chemotherapy and radiotherapy-naïve cancer patients. Int J Cardiovasc Imaging 34:1581–1587
33. Hatakenaka M, Yonezawa M, Nonoshita T, Nakamura K, Yabuuchi H, Shioyama Y, Nagao M, Matsuo Y, Kamitani T, Higo T, Nishikawa K, Setoguchi T, Honda H (2012) Acute cardiac impairment associated with concurrent chemoradiotherapy for esophageal cancer: magnetic resonance evaluation. Int J Radiat Oncol Biol Phys 83:e67–73
34. Haugnes HS, Wethal T, Aass N, Dahl O, Klepp O, Langberg CW, Wilsgaard T, Bremnes RM, Foss SD (2010) Cardiovascular risk factors and morbidity in long-term survivors of testicular cancer: a 20-year follow-up study. J Clin Oncol 28:4649–4657
35. Ma H, Jones KR, Guo R, Xu P, Shen Y, Ren J (2010) Cisplatin compromises myocardial contractile function and mitochondrial ultrastructure: role of endoplasmic reticulum stress. Clin Exp Pharmacol Physiol 37:460–465
36. van Kessel M, Seaton D, Chan J, Yamada A, Kermeen F, Hamilton-Craig C, Butler T, Sabapathy S, Morris N (2017) Erratum to: prognostic value of right ventricular free wall strain in pulmonary hypertension patients with pseudo-normalized tricuspid annular planesystolic excursion values. Int J Cardiovasc Imaging 33:585
37. Alghamdi MH, Mertens L, Lee W, Yoo SJ, Grosse-Wortmann L (2013) Longitudinal right ventricular function is a better predictor of right ventricular contribution to exercise performance than global or outflow tract ejection fraction in tetralogy of Fallot: a combined echocardiography and magnetic resonance study. Eur Heart J Cardiovasc Imaging 14:235–239
38. D'Andrea A, Stanziola A, D'Alto M, Di Palma E, Martino M, Scarafile R, Molino A, Rea G, Maglione M, Calabrò R, Russo MG, Bossone E, Saggar R (2016) Right ventricular strain: an independent predictor of survival in idiopathic pulmonary fibrosis. Int J Cardiol 222:908–910
39. Cavalcante JL, Rijal S, Althouse AD, Delgado-Montero A, Katz WE, Schindler JT, Crock F, Harinstein ME, Navid F, Gleason TG, Lee JS (2016) Right ventricular function and prognosis in patients with low-flow, low-gradient severe aortic stenosis. J Am Soc Echocardiogr 29:325–333